

1995

## Diffuse band profiles in the Rho Ophiuchi cloud

C Gregory Seab  
*University of New Orleans*

Theodore P. Snow

Follow this and additional works at: [https://scholarworks.uno.edu/phys\\_facpubs](https://scholarworks.uno.edu/phys_facpubs)



Part of the [Physics Commons](#)

---

### Recommended Citation

Astrophys. J. 443 698 (1995)

This Article is brought to you for free and open access by the Department of Physics at ScholarWorks@UNO. It has been accepted for inclusion in Physics Faculty Publications by an authorized administrator of ScholarWorks@UNO. For more information, please contact [scholarworks@uno.edu](mailto:scholarworks@uno.edu).

## DIFFUSE BAND PROFILES IN THE $\rho$ OPHIUCHI CLOUD

C. GREGORY SEAB

Department of Physics, University of New Orleans, Lakefront, New Orleans, LA 70148

AND

THEODORE P. SNOW, JR.

Center for Astrophysics and Space Astronomy, Campus Box 389, University of Colorado, Boulder, CO 80309

Received 1991 March 18; accepted 1994 October 24

### ABSTRACT

High-resolution, high signal-to-noise ratio line profiles are presented for the 5780 and 5797 Å diffuse interstellar bands toward six stars in the  $\rho$  Oph dark cloud. Target stars were chosen to exhibit a wide range of interstellar grain properties, as measured by grain polarization and far-UV extinction. The extreme case of the heavily reddened star HD 147889 is included; this star has one of the highest known  $\lambda_{\max}$  values, indicative of unusually large grains. Despite the differences in the grain properties, the line profiles and central wavelengths for the 5780 Å band were found to be essentially identical for all lines of sight. This finding is in contradiction to the results of the embedded cavity grain model for diffuse bands, which predicts changes in both profile and central wavelength with grain size and impurity concentration. Results therefore support a molecular origin for the diffuse bands.

*Subject headings:* dust, extinction — ISM: clouds — ISM: individual ( $\rho$  Ophiuchi Cloud) — line: profiles — stars: individual (HD 147889, SR 3)

### 1. INTRODUCTION

Diffuse interstellar bands (DIBs) were first recognized by Heger (1922) and identified as interstellar by Merrill (1934) six decades ago. The classic paper by Herbig (1975) lists 39 interstellar bands between 4430 Å and 6660 Å. A total of over 100 bands have been identified since by various authors (Sanner, Snell, & Vanden Bout 1978; Herbig & Soderblom 1982; Herbig 1988; Herbig & Leka 1991; Joblin et al. 1990; Tripp, Cardelli, & Savage 1994). Despite over half a century of study, the diffuse band carriers have not yet been positively identified. The current state of understanding of the diffuse bands will be summarized in the published proceedings of the recent conference in Boulder (Tielens & Snow 1995).

The essential features of the DIBs are that they exist in large numbers (over 100), vary in width from 0.35 Å to over 40 Å (Herbig 1975), show no rotational fine structure in high-resolution observations (e.g., Krelowski & Sneden 1993; Westerland & Krelowski 1988; Herbig & Soderblom 1982), have invariant wavelengths and profiles (cf. this paper), seem deficient in dark clouds (Adamson, Whittet, & Duley 1991) and in circumstellar environments (Waters et al. 1989; cf. however Le Bertre & Lequeux 1993), and vary in strength with respect to one another (e.g., McIntosh & Webster 1992) leading to attempts to classify the bands into families (Chlewicki et al. 1986; Josafatsson & Snow 1987; Krelowski & Walker 1987). Recent theories have favored large molecules of various sorts as the carriers of the diffuse bands. These include highly unsaturated hydrocarbons (Fulara et al. 1993; Webster 1992, 1993), ionized polycyclic aromatic hydrocarbons (PAHs) (Crawford, Tielens, & Allamandola 1985; Leger & d'Hendecourt 1985; van der Zwet & Allamandola 1985; Parisel, Berthier, & Ellinger 1992; Salama & Allamandola 1992; Snow 1992),  $C_{60}$  and other fullerenes (Kroto & Jura 1992; Webster 1992); and porphyrins (Johnson 1995). Small molecules are generally ruled out by the lack of observed rotational structure in the bands and the difficulty of preserving

such molecules against photodissociation in the diffuse interstellar medium (Smith, Snow, & York 1977). The older theory ascribing the DIBs to impurities within dust grains has generally lost favor because of its difficulties in fitting the observed band profiles (Chlewicki et al. 1986), but has not been altogether ruled out. This paper presents an observational test of the most recent version of the grain carrier hypothesis.

Grains were initially favored for the DIB carriers because of the large widths and lack of observable rotational structure in the band profiles, plus their evident ability to resist destruction in the harsh interstellar environment. The embedded cavity model of Purcell & Shapiro (1977) attributes the bands to resonantly absorbing impurity centers in small grains. This embedded cavity model predicted line profiles that are steeper on the red side and extended into absorption wings on the blue side. Sometimes the red side would have “emission” wings where the bulk absorption of the solid was reduced by the presence of the impurity. Observed profiles of narrow bands are either symmetric or have absorption wings extending to the red (Herbig & Soderblom 1982), contradicting the embedded cavity results. However, this model ignored the interaction between the resonant impurity and the host dielectric of the grain. More recently, Shapiro & Holcomb (1986a) have generalized the embedded cavity model to include this interaction as well as arbitrary particle sizes. This revised theory can match the observed profiles for an appropriate choice of grain parameters. The updated theory predicts certain line profile variations dependent on the size distribution of the grains. Shapiro & Holcomb (1986b, hereafter SH) make specific predictions for the nature of the profile variations to be seen in the  $\rho$  Oph dark cloud.

The  $\rho$  Oph dark cloud provides an excellent test for dust grain theories because there is a large variation of grain properties within the cloud. The wavelength  $\lambda_{\max}$  of maximum polarization shows an extreme range of sizes of the large grains (Savage & Mathis 1979; Serkowski, Mathewson, & Ford

1975); the variation of the far-UV extinction curve shows differences in the population of small grains (Mathis & Wallenhorst 1981). Snow, Timothy, & Saar (1982) use the cloud to look for variations in the line profile of the 4430 Å diffuse band. The present paper examines high-resolution, high signal-to-noise ratio profiles of the 5780 and 5797 Å diffuse bands in the  $\rho$  Oph cloud as a test of the grain origin hypothesis.

Section 2 below describes the observations, § 3 describes the data reduction and analysis, § 4 presents the results and discussion, and § 5 summarizes the conclusions.

## 2. OBSERVATIONS

Observations of the diffuse bands in the 5765–5890 Å region were done on the CFHT facility on Mauna Kea in two sessions on 1988 February 4–7 and 1989 September 14–16. The relatively strong, narrow diffuse bands at 5780 and 5797 Å were well placed for study. Additional bands at 5778, 5795, 5844, and 5849 Å are included in the region. The grating was set to include the sodium D lines at 5890 and 5896 Å as a check on the velocity structure of the clouds in the line of sight.

Data were recorded on the 1872 Reticon detector at coudé focus, using the 830 lines  $\text{mm}^{-1}$  grating with the blue optics train. This combination gives a dispersion of 4.8 Å  $\text{mm}^{-1}$  at the detector for a 2 pixel resolution of 0.14 Å, corresponding to 7  $\text{km s}^{-1}$  at 5780 Å. Very high signal-to-noise ratio levels can be reached with this system for modest exposure times, since the Reticon is readout-noise-limited and very stable over time. Signal-to-noise ratios of several hundred were typical for the present set of data, ranging from a high of 1500 for the bright star  $\zeta$  Oph to a low of 115 for the heavily reddened star HD 147889.

Targets in the  $\rho$  Oph cloud were selected to display as large a range of grain sizes as possible. The wavelength of maximum polarization  $\lambda_{\text{max}}$  was assumed to represent the general trend of grain sizes. The validity of this assumption is discussed in § 4. Values for  $\lambda_{\text{max}}$  ranged from 5550 Å for  $\sigma$  Sco, near the Galactic average, up to 8100 Å for HD 147889. The  $E(B-V)$  reddening values ranged from 1.33 mag for SR 3 to 0.20 mag for  $\beta^1$  Sco. Basic data for the target stars are given in Table 1, listed generally in order of increasing  $\lambda_{\text{max}}$ .

In addition to the CFHT data, high-dispersion (resolving power 55,000) spectra of the  $\rho$  Oph cloud star SR 3 were obtained at the Anglo-Australian Telescope (one of us [T. P. S.] spent the latter half of 1991 on sabbatical at the University of Sydney and the Anglo-Australian Observatory). SR 3 is an A0 star, first described by Struve & Rudkjøbing (1949), having visual magnitude 12.00 and  $E(B-V)$  color excess of 1.33. Its infrared colors and wavelength of maximum polarization indicate that this line of sight contains grains as large as any observed within the  $\rho$  Oph cloud (Carrasco, Strom, & Strom 1973). Therefore in SR 3 we have the longest

pathlength yet observed through the unusual environment of this cloud, and hence the best opportunity to detect any unusual optical effects brought about by the nature of the dust. These observations were carried as a service by Anglo-Australian Observatory staff astronomer Jason Spyromillio on 1991 May 31, using the University College London Echelle Spectrograph (UCLES) on the 4.0 m Anglo-Australian Telescope. A GEC CCD was the detector, providing a pixel size of 22  $\mu\text{m}$  in a 528  $\times$  1024 pixel array. Fourteen orders of the echelle spectrum were recorded at a resolving power (2 pixel) of 55,000.

## 3. DATA REDUCTION AND ANALYSIS

Data reduction for the CFHT data was done at the Regional Data Analysis Facility (RDAF) at the University of Colorado in Boulder.

Flat-field exposures at various exposure levels (ADCU counts) were obtained several times each night during the observation run. The Reticon detector was found to be sufficiently stable that the flat-field exposures did not change during the three nights of observing and were invariant for small (few Å) changes in the grating angle. Therefore, exposures from all three nights were averaged together to reduce the random noise in the flat fields. Some nonlinearity with exposure level is expected in the detector. To minimize this, flat fields were grouped according to exposure level as measured by the ADCU counts. Each target star exposure was then divided by the averaged flat field that most closely matched the general exposure level of the data. Matches to within  $\pm 20\%$  were possible in all cases.

Readout from the detector is interleaved on four separate channels. Small differences in the channels introduce a minor component of four-channel noise. This source of instrument noise can be reduced by averaging the exposure levels for every fourth pixel of the 1872, producing a separate average exposure level for each of the four channels. Data for each channel were then divided by the average for that channel, and the results reassembled into an 1872 pixel spectrum. While technically necessary, this procedure yielded little or no actual improvement in the noise levels of the spectrum. Wavelength calibration was done from a standard Fe/Ar discharge tube and reduced to a heliocentric scale. Figure 1 shows the diffuse band profiles for the CFHT target stars.

The data analysis for the SR 3 spectrum was performed at the Anglo-Australian Observatory in Epping, using the FIGARO analysis package. Biases were subtracted, flat fields divided out, and wavelength calibration applied before the four exposures (of 1000 s each) were co-added to produce the final spectrum shown in Figures 1 and 2.

Equivalent widths for the 5780 and 5797 Å features were measured with standard data reduction software available at the RDAF. The software incorporates manual choice of the continuum level on both sides, and a manual choice of the limits of the absorption feature. Note that the 5780 Å sharp feature (FWHM  $< 2.8$  Å; Herbig 1975) is superposed on a broad shallow feature centered 5778.3 Å (FWHM about 17 Å). For stars with strong diffuse bands, this produces a tilted continuum level, but should not effect the accuracy of the equivalent width measurements.

Table 2 shows the results of the equivalent width measurements for the program stars, along with two indicators of the grain size distribution: the wavelength  $\lambda_{\text{max}}$  of maximum polarization, and the level of the far-UV extinction. We note that the

TABLE 1  
BASIC STELLAR DATA

Name	HD	Spectral Type	$V$	$E(B-V)$
$\sigma$ Sco .....	147165	B1 III	8.29	0.39
$\omega^1$ Sco .....	144470	B1 V	3.96	0.22
$\beta^1$ Sco .....	144217	B1 V	2.62	0.20
$\rho$ Oph A.....	147933A	B2 IV	4.59	0.48
$\nu^1$ Sco.....	145502	B3 V	4.01	0.28
.....	147889	B2 V	7.90	1.10
SR 3 .....	...	A0	12.00	1.33

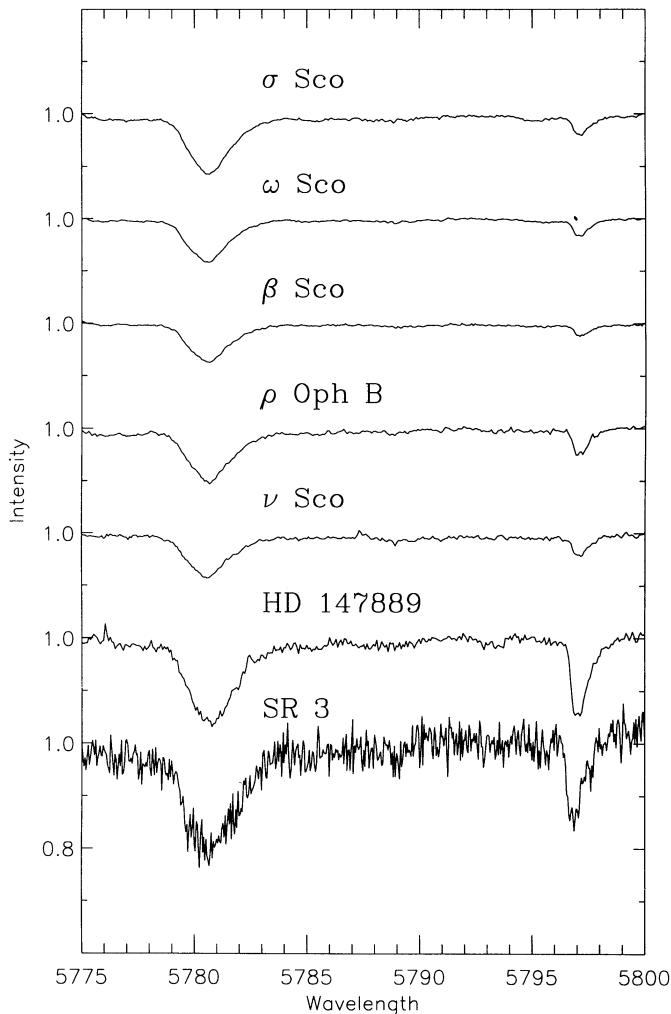


FIG. 1.—Normalized data for the target stars, showing the 5780 Å and 5797 Å diffuse interstellar bands. The stars are roughly in order of increasing  $\lambda_{\max}$ , ranging from 5500 Å for  $\sigma$  Sco to 8100 Å for HD 147889; the noisier spectrum of SR 3 ( $\lambda_{\max} = 8000$  Å) is placed at the bottom for clarity. Normalization is over the range 5765–5890 Å, so that the continuum level differs slightly from 1.0 for the stars.

equivalent widths for the 5780 Å band shown in Table 2 are generally lower than those measured by Snow & Cohen (1974) and compiled by Snow, York, & Welty (1977). These previous measurements were relatively low signal-to-noise ratio, low-resolution observations as compared to the present results.

TABLE 2  
GRAIN SIZE INDICATOR AND BAND EQUIVALENT WIDTH (Å)

Name	HD	$\lambda_{\max}$ (Å) <sup>a</sup>	Far UV <sup>b</sup>	$W_{\lambda}(5780)$	$W_{\lambda}(5797)$
$\sigma$ Sco .....	147165	5500	3.6	0.230	0.035
$\omega^1$ Sco .....	144470	5950	11.1	0.168	0.032
$\beta^1$ Sco .....	144217	6100	10.4	0.136	0.016
$\rho$ Oph A .....	147933	6900	5.1	0.207	0.053
$\nu^1$ Sco .....	145502	7100	8.1	0.175	0.037
... .....	147889	8100	7.2 <sup>c</sup>	0.345	0.158
SR 3 .....	...	8000	...	0.397	0.098

<sup>a</sup> Polarization data from Carrasco et al. 1973. Average interstellar value is 5450 Å.

<sup>b</sup>  $E(1135 - V)/E(B - V)$  from Snow & Jenkins 1980, except as noted.

<sup>c</sup> Measured from data in Seab 1982.

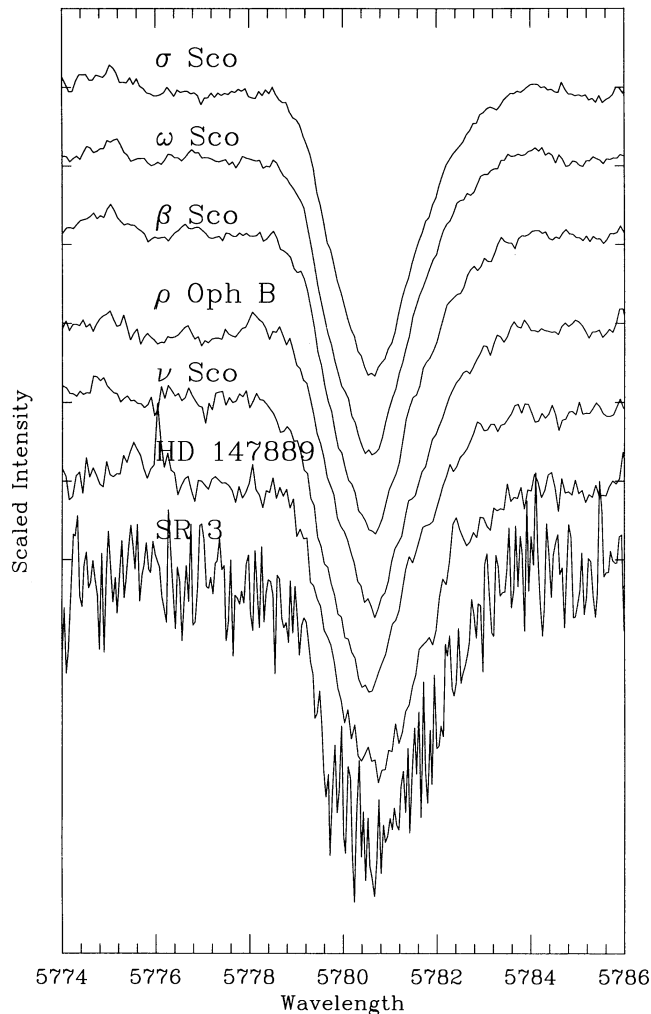


FIG. 2.—Comparison of the 5780 Å line profiles for the  $\rho$  Oph cloud stars. The lines have been normalized to the same continuum level and central depth. The line profiles are identical to within the noise limits of the data.

The high signal-to-noise ratio, high-resolution results presented in Table 2 should be preferred to the older measurements in every case.

## 4. RESULTS AND DISCUSSION

### 4.1. Grain Size in the $\rho$ Oph Cloud

One reason for studying stars in the  $\rho$  Ophiuchi cloud is that the properties of the dust grains vary widely within the cloud; in particular, the sizes of the dust grains are known to vary considerably. The usual measure of the “typical” size of the grains is the polarization parameter  $\lambda_{\max}$ , which varies in the  $\rho$  Oph cloud from 8100 Å down to 5550 Å, close to the interstellar average of 5450 Å (Carrasco et al. 1973; Serkowski et al. 1975). A strong correlation exists between  $\lambda_{\max}$  and  $R$ , the ratio of selective to total extinction; these indicators are usually assumed to imply a larger than normal grain size distribution in the line of sight (Serkowski et al. 1975). Since this is based on optical polarization measurements, it yields information specifically on those polarizing grains that also produce the optical extinction. It does not give any direct information on other large grains that do not produce polarization, nor does it say anything about the population of small grains. Neverthe-

less, it is reasonable to assume that the processes that increase the size of the polarizing grains will also effect the non-polarizing large grains.

It is often assumed that the small grains are also larger in the lines of sight with large  $\lambda_{\max}$ . For example, SH make this assumption in calculating grain profiles for the  $\rho$  Oph cloud. This is, however, only an assumption and may not be a good one. In the case of  $\sigma$  Sco, UV extinction data demonstrate that the small grains do not necessarily follow the growth pattern of the large grains. This star has one of the lowest far-UV extinction curves known (Bless & Savage 1972). Since small (50–500 Å) grains are thought to be responsible for the normal far-UV extinction rise, the absence of the rise generally indicates an absence of small grains (Mathis & Wallenhorst 1981; Seab & Snow 1989). This is in contrast to a near-normal  $\lambda_{\max}$  value of 5550 Å, the lowest of the  $\rho$  Oph stars included in this study. Mathis & Wallenhorst (1981) show that the UV extinction of  $\sigma$  Sco can be fitted by increasing the lower size limit on the grains in the standard model of Mathis, Rumpl, & Nordsieck (1977), so that the population is deficient in small grains but retains a normal population of large grains. They also fitted the  $\rho$  Ophiuchi line of sight by increasing both the upper and lower size limits on the grain population, in agreement with the large  $\lambda_{\max}$  and low far-UV extinction.

The availability of UV extinction data for many of the stars in the  $\rho$  Oph cloud (Seab 1982; Snow & Jenkins 1980; Wu, Gilra, & Van Duinen 1980) provides a more direct measure of the relative population of small grains. However, some care must be exercised in the interpretation of the far-UV extinction data. As Joseph et al. (1986) point out, a small increase in the sizes of the small grains, as would happen with accretion proportional to the surface area, actually *raises* the far-UV extinction level. A low far-UV extinction, then, is indicative of a significantly reduced population of the smallest grains. This can be achieved by destroying the small grains, coagulating them onto large grains, or accreting enough material to make them into medium-sized or larger grains as in the Mathis & Wallenhorst (1981) model.

The very small grains (VSGs) or polycyclic aromatic hydrocarbons (PAHs) that have been suggested as the carriers of the diffuse interstellar bands (van der Zwet & Allamandola 1985; Leger & d'Hendecourt 1985; Crawford et al. 1985) are not major contributors to either the UV or the optical extinction, so that it is difficult to quantify any changes in the population of these very small grains or very large molecules.

Despite these limitations, the known variations in grain properties in the  $\rho$  Oph cloud make it a good candidate for diffuse band studies.

#### 4.2. Diffuse Band Profiles

SH have used the  $\rho$  Oph cloud stars to make specific predictions of changes in the diffuse band profiles based on the sizes of the grains as measured by  $\lambda_{\max}$ . Their embedded cavity theory, an application of Purcell & Shapiro (1977) as extended by Shapiro & Holcomb (1986a), attributes diffuse bands to resonantly absorbing impurity atoms or molecules within grains. One feature of this theory is that the profile of the band depends on the host grain size and composition, on the impurity oscillator strength and concentration, and on the presence or absence of grain mantles. They found that an appropriate choice of parameters could be found to fit the observed band profiles from Herbig & Soderblom (1982) for the 6613 Å band, and from Snell & Vanden Bout (1981) for the 5780 Å band.

Applying the theory to the larger grain sizes appropriate to the stars in the  $\rho$  Oph cloud, SH predict the appearance of “blue emission wings” in the 5780 Å band profile for the stars with the largest grains. Note the “emission wing” is a misnomer for these features, since they do not involve any emission, but only mimic an emission feature by reducing the extinction in the wing to a value below that of the bulk material without the embedded cavity.

The 5780 Å band profiles presented in Figure 1 do not show the predicted blue emission wings, even in the extreme cases of HD 147889 and SR 3. Figure 2 presents a direct comparison of the 5780 Å band profiles for all of the target stars, ordered roughly with increasing  $\lambda_{\max}$  (SR 3 is placed last because it was taken with a different instrument and has a lower S/N ratio). The bands in all of these stars are essentially identical to within the limits of the noise. Neither is there any systematic variation correlated to the far-UV extinction measure given in Table 1. Concurrent observations of the sodium D lines at 5890, 5896 Å show no evidence of velocity components able to obscure the expected emission wings. The Shapiro & Holcomb prediction is not borne out by the data.

SH mention three possible conclusions in the case that the predicted profile variations are not seen:

1. The band carrier grains do not vary in size in the same way as the polarizing grains do (or, in this analysis, with the small grains producing the far-UV extinction).
2. The relative contributions of polarizing grains versus band carrier grains changes with  $\lambda_{\max}$  (and/or the far-UV extinction).
3. Grains are not the band carriers.

Consideration of these caveats means that the embedded cavity model is not rigorously excluded by these results, but we will argue that the first two possibilities are unlikely to provide an adequate explanation for the lack of band profile variations.

The fact that the band profiles do not vary at all from star to star within the  $\rho$  Oph cloud places a stronger restriction on the nature of the carriers than statement (1) above. The lack of observed blue emission wings constrains the carrier grains in the SH model to remain small in all cases ( $x = 2\pi\lambda/r < 1$ ), independent of what the other grains in the line of sight are doing. Since the  $\rho$  Oph cloud is remarkable for the large variations in grain properties in the various stars, it would be surprising to find that there was one population of grains that remained constant while other populations changed. It is still possible, however, that the grain carriers are so small that they remain within the small particle limit even with grain growth. In this case, one would still expect a change in DIB strength correlated with the number population of small grains as reflected by the far-UV extinction curve. This correlation would be expected whether or not the DIB carrier grains are the same as those giving the bulk of the far-UV extinction, since the coagulation of small grains onto large ones should not be sensitive to the grain type. Table 2 shows no such effect. For example,  $\sigma$  Sco and  $\beta$  Sco differ widely in their far-UV extinction values, but have essentially identical  $W_\lambda(5780)/E(B-V)$  parameters. We conclude that statement (1) above is not a reasonable explanation for the lack of DIB profile variations both from the lack of profile variations and relative band strengths.

It would likewise be remarkable to find that the relative contribution of carrier grains and polarizing grains to the observed  $E(B-V)$  changed with  $\lambda_{\max}$  in just such a fashion to

cancel out any effects on the band profiles. This would seem to require a fairly specialized type of variation in grain properties. We conclude that while the present data do not rigorously exclude the embedded carrier model of the diffuse bands, they do seriously constrain it.

As a further note, the central wavelengths of the bands are seen in Figure 2 to remain constant. While SH do not make any specific predictions of the behavior of the location of the bands, their method of calculation solves for the difference between the observed  $\lambda_c$  and the wavelength  $\lambda_0$  corresponding to the natural frequency of the impurity resonance. Since they fix the observed wavelength, this difference shows up as variations in the  $\lambda_0$  values in their Table 2. A glance at this table shows differences of up to 8 Å (for their cases 4a and 6a) in the wavelength. For real grains, one would expect that  $\lambda_0$  would be fixed by the impurity/host combination, so that the variation would be reflected in the observed central wavelength  $\lambda_c$  values. No such differences are seen in the  $\rho$  Oph data, again reinforcing the conclusion that the diffuse band carriers do not participate in the large variations in grain properties otherwise evident in this cloud.

If the embedded cavity model is correct, then the carrier grains cannot be any of the following: small grains (excluded by the discussion above); large grains (excluded for  $x > 1$  by SH); grain material with large dielectric constant such as graphite and magnetite (also excluded by SH); any grains that participate in the general size increase noted in the  $\rho$  Oph cloud (excluded by present observations); and any grains that change in such a manner as to shift the central wavelength of the band (also by present observations). One wonders what band carrier candidates are left. Conceivably, one could have the carriers be small silicate grains within an aggregate model like that suggested by Seab (1988) or Mathis & Whiffen (1989), but even so, it is difficult to see how the size changes that result in the increase in  $\lambda_{\max}$  would not similarly affect the band optical properties.

The similarity of the band profiles shown in Figure 2 is remarkable, given the wide variation of grain properties in the lines of sight. The profiles are essentially identical to within the noise limit of the spectra. The noisiest spectra, that of SR 3, was

taken with a completely different instrument, but still shows the same profile and central wavelength. This similarity in profiles is a strong argument that the diffuse bands do not depend in any significant way on the size distribution of the grain population.

#### 4.3. Band Strength Correlations

Figure 3a shows that the ratio of the 5780 Å diffuse band equivalent widths to the  $E(B-V)$  reddening grows distinctly weaker with depth in the  $\rho$  Oph cloud, in accord with the finding of Snow & Cohen (1974) for DIBs in dark clouds, and of Adamson et al. (1991) for the Taurus dark cloud. This decrease in the production efficiency of the band in the interior of the clouds also produces an apparent nonzero intercept in the  $W_\lambda$  versus  $E(B-V)$  correlation, as found by Snow et al. (1977) and Herbig (1975). Figure 3b shows this correlation for the program stars; also shown is the best-fit line from the diffuse band compilation of Snow et al. (1977), and the least-squares best fit from the present data. The best-fit line through the present data nearly parallels the Snow et al. (1977) fit, although with a smaller intercept, consistent with the smaller DIB equivalent widths measured from modern high S/N data as compared to the photographic measurements in the older data (e.g., Snow & Cohen 1974 DIB measurements for the  $\rho$  Oph cloud stars). Herbig (1993) and Webster (1993) show that the nonzero intercept is not real but is apparently a consequence of the weakening production efficiency of the bands in clouds. Reinforcing this pattern is the extreme case of a weak 5780 Å diffuse band toward HD 29647 in the Taurus cloud found by Snow & Seab (1991).

The relative weakening of the 5780 Å DIB in dark clouds, combined with the lack of variation in the profile and central wavelength of the band, sets some general constraints on the nature of the carriers. Grain carrier theories are not very consistent with these observations. Although the band strength could potentially be decreased by mantling the grains with ice or impurity-free material, one would expect that the band profile and/or central wavelength would also be changed (SH). Theories based on partially hydrogenated molecules (e.g., Webster 1993; Fulara et al. 1993) are consistent in that they

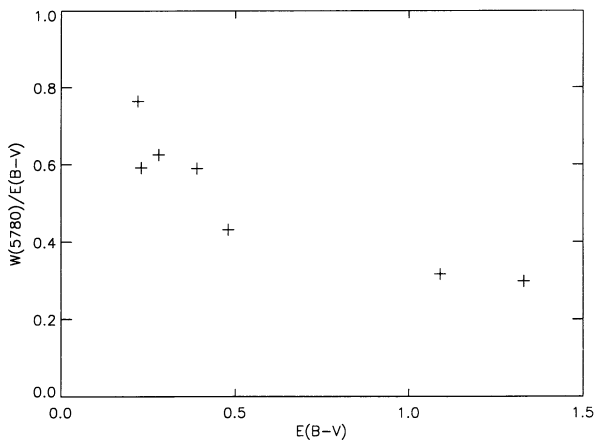


FIG. 3a

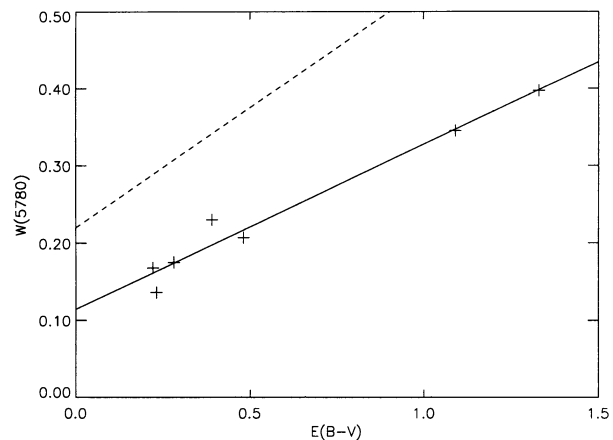


FIG. 3b

FIG. 3.—(a) Relative strength of the 5780 Å band  $W_\lambda/E(B-V)$  as a function of  $E(B-V)$  reddening in the  $\rho$  Oph cloud. Here, the “production efficiency” of the band appears weaker as the depth in the cloud increases. (b) Equivalent width  $W_\lambda$  of the 5780 Å diffuse band directly as a function of  $E(B-V)$  reddening in the cloud. The dashed line is the average interstellar fit from Snow et al. (1977):  $W_\lambda = 0.31 E(B-V) + 0.22$ ; the solid line is from the present small data set:  $W_\lambda = 0.21 E(B-V) + 0.116$ .

assume the increased degree of hydrogenation expected in dark clouds suppresses the bands. Ionized molecule theories (e.g., Parisel et al. 1992; Salama & Allamandola 1992; Crawford et al. 1985) are similarly consistent with these observations under the assumption that the ionized carriers recombine to a neutral (non-DIB-producing) state within the dark clouds. However, we note that these carriers must also satisfy the observation that DIBs are generally not observed in circumstellar environments (Snow & Wallerstein 1972; Snow 1973; Waters et al. 1989; cf., however, Le Bertre & Lequeux 1993).

The 5797 Å band does not share the same clear behavior as the 5780 Å band; Figure 4 shows a more random pattern for this band. The difference between the two bands clearly illustrates the conclusion that these two diffuse bands must have separate origins (Krelowski & Westerlund 1988) and contradicts the grouping of 5780 and 5797 bands into the same family by Josafatsson & Snow (1987). It is equally clear that the variation in the relative strengths of the 5780 and 5797 Å bands are not correlated with cloud density as argued by McIntosh & Webster (1992) on the basis of data from the Taurus dark cloud. Figure 5 presents the ratio of the strengths of these bands as a function of  $\lambda_{\max}$ ; this figure compares to Figure 1 from McIntosh & Webster (1992), making use of the fact that  $R$  correlates very well with  $\lambda_{\max}$  and that the 5780 band Å dominates Family 2 of Krelowski & Walker (1987), while the 5797 Å band dominates Family 3. McIntosh & Webster (1992) showed an increase in the ratio of the Family 2 to Family 3 bands with respect to  $R$ , interpreted to mean that the Family 2 bands extend deeper in to the cloud and bears more hydrogen atoms on the hydrocarbon molecule than the Family 3 bands. Here we see the exact opposite relationship: the  $W(5780)/W(5797)$  ratio decreases with respect to  $\lambda_{\max}$ ; nor is there any good correlation of this ratio with either the far-UV extinction  $E(1135 - V)/E(B - V)$  or with the absolute extinction  $A_{1135}$ . It would be interesting to check if the correlation with CH and CN abundances found by Krelowski et al. (1992) holds for these  $\rho$  Oph cloud stars.

The above result illustrates the danger inherent in drawing positive conclusions based on a limit sample of target stars, particularly when the stars are all in the same cloud. Negative conclusions, such as those found in this paper, are all right, but the occasional practice of generalizing trends from single-cloud studies has to be suspect. For example, we find in Figure 6 that

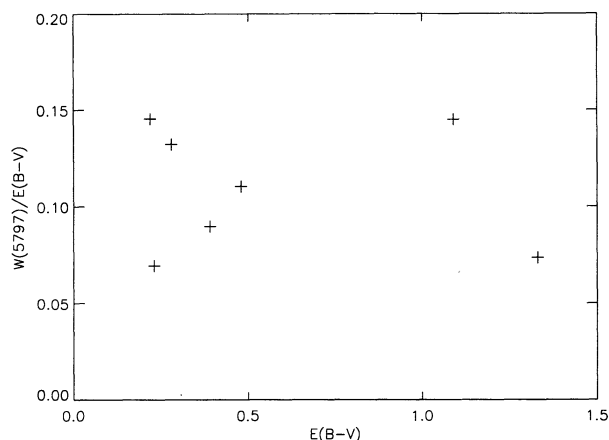


FIG. 4.—Equivalent width  $W_{\lambda}$  of the 5797 Å band as a function of reddening in the  $\rho$  Oph cloud, as in Fig. 3a.

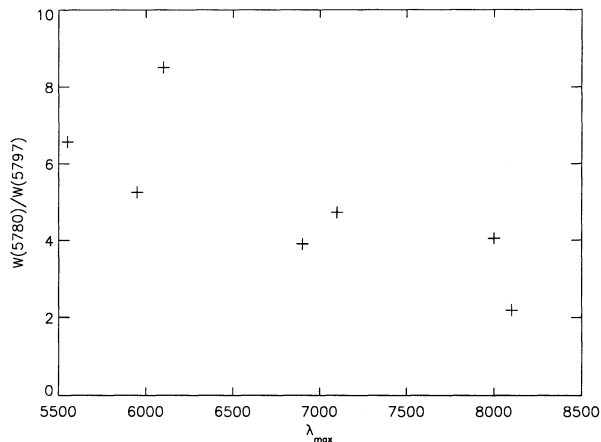


FIG. 5.—The ratio of equivalent widths of the 5780 Å and 5797 Å bands as a function of the wavelength of maximum polarization. Compare these results to those of McIntosh & Walker (1992) for the Taurus cloud stars.

the correlation in  $\rho$  Oph between the percentage polarization (Carrasco et al. 1973) and the strength of the 5780 Å band is as strong as any correlation found. The interpretation of this finding is not clear and may be simply a consequence of correlations of each quantity with other things.

## 5. CONCLUSIONS

Diffuse band data are presented for a number of lines of sight in the  $\rho$  Ophiuchi cloud exhibiting different interstellar grain properties. No systematic changes in the 5780 Å diffuse band profile are seen for a wide range of grain size parameters. The lines of sight vary significantly in both  $\lambda_{\max}$ , the wavelength of maximum polarization, and in the far-UV extinction level. The former is taken as an indicator of the sizes of large grains, while the latter refers to the population of small grains. The lack of systematic profile changes argues against the embedded cavity grain model for diffuse bands, and specifically contradicts the predictions of diffuse emission wings in lines of sight with large grains as made by SH. While this model is not rigorously excluded, it is severely constrained by the observations presented herein.

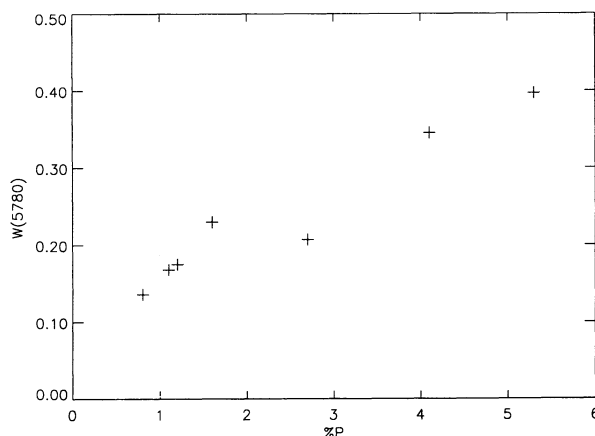


FIG. 6.—The correlation of 5780 Å DIB strength with the percentage polarization from Carrasco et al. (1973).

The production efficiency of the 5780 Å diffuse band strength decreases systematically with depth in the cloud. The ratio of the 5780 and 5797 Å bands is found to decrease with increasing  $\lambda_{\text{max}}$ , in contrast to the trend found for the Taurus dark cloud. No strong correlations with other quantities are found for these bands in the  $\rho$  Oph cloud stars.

This research has been supported by NSF grant NSF/LaSER (1989)-RFAP-08 to the University of New Orleans, and by NSF grant AST 85-05587 to the University of Colorado. We are grateful for the access to the Canada-France-

Hawaii Telescope provided through the courtesy of the Canadian National Research Council, and for the observing assistance provided by Jean Arnaud and Tom Gregory of the CFHT staff. Data reduction and analysis assistance was provided by Krista Lawrance and Robert Rudloff at the University of Colorado. Jim Boyd did final data reduction tasks and helped produce the figures. T. P. S. gratefully acknowledges the hospitality of the University of Sydney and the Anglo-Australian Observatory, and the assistance of J. Spyromillio of the AAO, who obtained the data during service observing time, and who helped with the data reduction on SR 3.

## REFERENCES

- Adamson, A. J., Whittet, D. C. B., & Duley, W. W. 1991, *MNRAS*, 252, 234  
 Bless, R. C., & Savage, B. D. 1972, *ApJ*, 171, 293  
 Carrasco, L., Strom, S. E., & Strom, K. M. 1973, *ApJ*, 182, 95  
 Chlewicki, G., van der Zwet, G. P., van Ijendoorn, L. J., Greenberg, J. M., & Alvarez, P. P. 1986, *ApJ*, 305, 455  
 Crawford, M. K., Tielens, A. G. G. M., & Allamandola, L. J. 1985, *ApJ*, 293, L45  
 Fulara, J., Lessen, D., Freivogel, P., & Maier, J. P. 1993, *Nature*, 366, 439  
 Heger, M. L. 1922, *Lick Obs. Bull. No. 337*, 10  
 Herbig, G. H. 1975, *ApJ*, 196, 129  
 ———. 1988, *ApJ*, 331, 999  
 ———. 1993, *ApJ*, 407, 142  
 Herbig, G. H., & Leka, K. D. 1991, *ApJ*, 382, 193  
 Herbig, G. H., & Soderblom, D. R. 1982, *ApJ*, 252, 610  
 Joblin, C., Maillard, J. P., d'Hendecourt, L., & Leger, A. 1990, *Nature*, 346, 729  
 Johnson, F. 1995, in *The Diffuse Interstellar Bands*, ed. A. G. G. M. Tielens & T. P. Snow (Dordrecht: Kluwer), in press  
 Josafatsson, K., & Snow, T. P. 1987, *ApJ*, 319, 436  
 Joseph, C. L., Snow, T. P., Seab, C. G., & Crutcher, R. M. 1986, *ApJ*, 309, 771  
 Krelowski, J., & Sneden, C. 1993, *PASP*, 105, 1141  
 Krelowski, J., Snow, T. P., Seab, C. G., & Papaj, J. 1992, *MNRAS*, 258, 693  
 Krelowski, J., & Walker, G. A. H. 1987, *ApJ*, 312, 860  
 Krelowski, J., & Westerlund, B. E. 1988, *A&A*, 190, 339  
 Kroto, H. W., & Jura, M. 1992, *A&A*, 263, 275  
 Le Bertre, T., & Lequeux, J. 1993, *A&A*, 274, 909  
 Leger, A., & d'Hendecourt, L. B. 1985, *A&A*, 146, 81  
 Mathis, J. S., Ruml, W., & Nordsieck, K. H. 1977, *ApJ*, 217, 425  
 Mathis, J. S., & Wallenhorst, S. G. 1981, *ApJ*, 244, 483  
 Mathis, J. S., & Whiffen, G. 1989, *ApJ*, 341, 808  
 McIntosh, A., & Webster, A. 1992, *MNRAS*, 255, 37P  
 Merrill, P. W. 1934, *PASP*, 46, 206  
 Parisel, O., Berthier, G., & Ellinger, Y. 1992, *A&A*, 266, L1  
 Purcell, E. M., & Shapiro, P. R. 1977, *ApJ*, 214, 92  
 Salama, F., & Allamandola, L. J. 1992, *ApJ*, 395, 301  
 Sanner, F., Snell, R., & Vanden Bout, P. 1978, *ApJ*, 226, 460  
 Savage, B. D., & Mathis, J. M. 1979, *ARA&A*, 17, 73  
 Seab, C. G. 1982, Ph.D. thesis, Univ. of Colorado, Boulder  
 ———. 1988, in *Dust in the Universe*, ed. M. E. Baily & D. A. Williams (Cambridge: Cambridge Univ. Press), 303  
 Seab, C. G., & Snow, T. P. 1989, *ApJ*, 347, 479  
 Serkowski, K., Mathewson, D. S., & Ford, V. L. 1975, *ApJ*, 196, 261  
 Shapiro, P. R., & Holcomb, K. A. 1986a, *ApJ*, 305, 433  
 ———. 1986b, *ApJ*, 310, 872 (SH)  
 Smith, W. H., Snow, T. P., & York, D. G. 1977, *ApJ*, 218, 124  
 Snell, R. L., & Vanden Bout, P. A. 1981, *ApJ*, 244, 844  
 Snow, T. P. 1973, *PASP*, 85, 590  
 ———. 1992, *ApJ*, 401, 775  
 Snow, T. P., & Cohen, J. G. 1974, *ApJ*, 194, 313  
 Snow, T. P., & Jenkins, E. B. 1980, *ApJ*, 241, 161  
 Snow, T. P., & Seab, C. G. 1991, *ApJ*, 382, 189  
 Snow, T. P., Timothy, J. G., & Saar, S. 1982, *ApJ*, 262, 611  
 Snow, T. P., & Wallerstein, G. 1972, *PASP*, 84, 492  
 Snow, T. P., York, D. G., & Welty, D. E. 1977, *AJ*, 82, 113  
 Struve, O., & Rudkjobing, M. 1949, *ApJ*, 109, 92  
 Tielens, A. G. G. M., & Snow, T. P., ed. 1995, *The Diffuse Interstellar Bands* (Dordrecht: Kluwer), in press  
 Tripp, T. M., Cardelli, J. A., & Savage, B. D. 1994, *AJ*, 107, 645  
 van der Zwet, G. P., & Allamandola, L. J. 1985, *A&A*, 146, 76  
 Waters, L. B. F. M., et al. 1989, *A&A*, 211, 208  
 Webster, A. 1992, *MNRAS*, 255, 41P  
 ———. 1993, *MNRAS*, 262, 831  
 Westerlund, B. E., & Krelowski, J. 1988, *A&A*, 203, 134  
 Wu, C.-C., Gilra, D. P., & Van Duinen, R. J. 1980, *ApJ*, 241, 173